Colder Eastern Equatorial Pacific and Stronger Walker Circulation in the Early 21st Century: Separating the Forced Response to Global Warming From Natural Variability

Ulla Heede, Alexey V. Fedorov

Geophysical Research Letters

RESEARCH LETTER
10.1029/2022GL101020

Colder Eastern Equatorial Pacific and Stronger Walker Circulation in the Early 21st Century: Separating the Forced Response to Global Warming From Natural Variability

Ulla K. Heede[1,2] **and Alexey V. Fedorov**[1,3]

[1]Department of Earth and Planetary Sciences, Yale University, New Haven, CT, USA, [2]Cooperative Institute for Research in Environmental Sciences, University of Colorado, Boulder, CO, USA, [3]LOCEAN/IPSL, Sorbonne University, Paris, France

Key Points:

- A multi-decadal strengthening of the Pacific Walker cell is observed in a wide range of indices, especially after 1990
- A Northern Hemisphere - Indo West Pacific warming sea surface temperature pattern, which differs from the Pacific Decadal Oscillation, is evident since 1980
- This pattern resembles a forced response to abrupt CO_2 forcing, emerging in a subset of climate models, and contributes to the Walker circulation strenthening

Supporting Information:

Supporting Information may be found in the online version of this article.

Correspondence to:

U. K. Heede,
ulla.heede@colorado.edu

Citation:

Heede, U. K., & Fedorov, A. V. (2023). Colder eastern equatorial Pacific and stronger Walker circulation in the early 21st century: Separating the forced response to global warming from natural variability. *Geophysical Research Letters*, *50*, e2022GL101020. https://doi.org/10.1029/2022GL101020

Received 31 AUG 2022
Accepted 5 JAN 2023

Author Contributions:

Conceptualization: Ulla K. Heede, Alexey V. Fedorov
Formal analysis: Ulla K. Heede
Funding acquisition: Ulla K. Heede, Alexey V. Fedorov
Methodology: Ulla K. Heede, Alexey V. Fedorov
Software: Ulla K. Heede
Supervision: Alexey V. Fedorov
Visualization: Ulla K. Heede
Writing – original draft: Ulla K. Heede

Abstract Since the early 1990s the Pacific Walker circulation shows a multi-decadal strengthening, which contradicts future model projections. Whether this trend, evident in many climate indices especially before the 2015 El Niño, reflects the coupled ocean-atmosphere response to global warming or the negative phase of the Pacific Decadal Oscillation (PDO) remains debated. Here we show that sea surface temperature trends during 1980–2020 are dominated by three signals: a spatially uniform warming trend, a negative PDO pattern, and a Northern Hemisphere-Indo-West Pacific warming pattern. The latter pattern, which closely resembles the transient ocean thermostat-like response to global warming emerging in a subset of CMIP6 models, shows cooling in the central-eastern equatorial Pacific but warming in the western Pacific and tropical Indian Ocean. Together with the PDO, this pattern drives the Walker circulation strengthening in the equatorial band. Historical simulations appear to underestimate this pattern, contributing to the models' inability to replicate the Walker cell strengthening.

Plain Language Summary This paper investigates the observed changes in the tropical Pacific during the satellite era, including the recent decadal strengthening of the atmospheric zonal circulation—the Walker cell. We aim to understand the extent to which these changes represent a forced response to rising CO_2 concentrations versus natural variability. We apply an approach in which we decompose the observed sea surface temperature trends into three components—a pattern associated with the Pacific Decadal Oscillation, which is part of natural variability, a uniform warming pattern, and a residual pattern. This residual pattern shows a remarkable resemblance to a forced ocean thermostat-like transient response generated in some of the climate models, characterized by equatorial Pacific (EP) cooling, and a broad warming of the Northern Hemisphere, and the Indian Ocean and West Pacific. These results challenge studies arguing that the recent strengthening of the Pacific Walker cell can be explained simply by multi-decadal natural variability in the tropics. Furthermore, the inability of climate models at large to fully capture this forced pattern with historical forcing puts into focus the reliability of future projections of climate change in the tropical Pacific, specifically the timing of emergence of the eastern EP warming.

1. Introduction

The tropical Pacific modulates the global climate on a broad range on timescales. The easterly trade winds drive equatorial upwelling, whose strength is controlled by atmospheric zonal circulation—the Pacific Walker cell. The Walker cell is in turn coupled to the equatorial Pacific (EP) east–west sea surface temperature (SST) gradient via the Bjerknes feedback (Bjerknes, 1969). Variations in the strength of the Walker cell on interannual timescales play a key role in the El Niño Southern Oscillation (ENSO) phenomenon (e.g., McPhaden et al., 2020), while on decadal timescales control the Pacific Decadal Oscillation (PDO) (Mantua et al., 1997; Newman et al., 2016; Y. Zhang et al., 1997). Both ENSO and the PDO can modulate the rates of surface mean temperature increase associated with global warming (England et al., 2014; Hu & Fedorov, 2018; Kosaka & Xie, 2016). Furthermore, the Pacific Walker circulation is sensitive to external forcing both on geological timescales (Fedorov et al., 2015; Shankle et al., 2021; Wara, 2005) and with contemporary climate change (e.g., DiNezio et al., 2009; Heede et al., 2020, 2021; Heede & Fedorov, 2021; Knutson & Manabe, 1995).

The majority of General Circulation Models (GCMs) participating in the Coupled Model Intercomparison Project (CMIP) indicate that the Pacific Walker cell will slow down in response to increasing radiative forcing, which will be accompanied by the establishment of the eastern EP warming pattern (Coats & Karnauskas, 2017;

Writing – review & editing: Ulla K. Heede, Alexey V. Fedorov

DiNezio et al., 2009, 2012; Heede & Fedorov, 2021; Kociuba & Power, 2015; Xie et al., 2010). The weakening of the Walker circulation can be explained by several, often interconnected mechanisms. Specifically, energetic constraints imply reduced atmospheric vertical mass flux with global warming as specific humidity increases faster than precipitation (Held & Soden, 2006; Vecchi & Soden, 2007) even though the surface manifestation of this effect in the Pacific varies in climate GCMs (Heede et al., 2021) and is affected by changes in precipitation efficiency (Li et al., 2022, 2023). Other factors include greater effective static stability over ascending regions (Chou et al., 2009; Knutson & Manabe, 1995; Wills et al., 2017); the lesser ability of the colder eastern Pacific to balance increased radiative forcing by evaporative cooling compared to the warmer western Pacific (Heede et al., 2020; Knutson & Manabe, 1995; Merlis & Schneider, 2011); positive marine boundary layer cloud feedbacks in the eastern Pacific (Erfani & Burls, 2019); and enhanced extra-tropical warming and/or slowdown of the oceanic subtropical cells (Burls & Fedorov, 2014; Heede et al., 2020, 2021; Sun et al., 2004).

These results have motivated studies looking for a similar eastern EP warming pattern and Walker circulation slowdown in the observed record. Several studies argued that the Walker cell may have shown a weakening trend throughout the 20th century (Tokinaga et al., 2012; Vecchi et al., 2006). However, other studies suggest that the Pacific east–west SST gradient has actually increased over the 20th century (Seager et al., 2019; Solomon & Newman, 2012). During the satellite era, when data uncertainties are greatly reduced, a robust multi-decadal strengthening of Pacific trade winds has been observed (Meng et al., 2012; Sohn et al., 2013; Y. Luo et al., 2015; Ma & Zhou, 2016).

This apparent discrepancy between future projections and the recently observed trends, and the inability of CMIP models to capture the observed trends, has brought the robustness of the future projections of a weaker Walker cell into question (Kociuba & Power, 2015; Seager et al., 2022). Another related question has emerged: does the observed trend reflect the negative phase of the PDO—a component of natural climate variability which the models do not necessarily simulate accurately (Douville et al., 2015; McGregor et al., 2018) and whose positive and negative phases alternate randomly with limited predictability? Several studies have argued that natural Pacific decadal variability may indeed play a role in the current trends and explain a part of the observed trend (Chung et al., 2019; Watanabe et al., 2020; Wu et al., 2021).

In parallel, other studies suggest that the strengthening of the Walker cell could be part of the forced response to global warming, akin to the ocean thermostat mechanism first proposed by Clement et al. (1996), Sun and Liu (1996), and Seager and Murtugudde (1997). In Clement et al. (1996), for example, a stronger upwelling in the eastern EP balances radiative fluxes induced by rising greenhouse gas concentrations, keeping the east colder than the west. Using a similar model (Seager et al., 2019) argues that such a forced thermostat-type response may be indeed consistent with the observed trends. However, in contrast to the original ideas of Clement et al. (1996) who used the Zebiak-Cane model (1987) with a fixed oceanic mean state, Heede et al. (2020, 2021) argue that this ocean thermostat is likely a transient phenomenon because the subsurface ocean will gradually warm thus limiting the effect of enhanced upwelling. As they show in idealized GCM simulations, this transient response can maintain a stronger Walker cell for about half-a-century or longer depending on the rate of change of the forcing (abrupt vs. gradual). In realistic global warming scenarios, this effect may lead to a multi-decadal delay in the weakening of the Walker cell (Heede & Fedorov, 2021). Additionally, nudging Indian ocean temperatures toward the observations in a GCM strengthens the Pacific Walker cell in Zhang et al. (2019), consistent with earlier results of J.-J. Luo et al. (2012). Together, these findings suggest that the current trends may reflect a transient ocean-thermostat-like (OT) forced response to global warming, in which the western EP and the Indian Ocean warm faster than the central-eastern Pacific, strengthening the Walker circulation.

Other studies suggest that the stronger Pacific Walker cell may be ultimately driven by the warming of the tropical Atlantic (Hu & Fedorov, 2018; Kucharski et al., 2011; Levine et al., 2017; McGregor et al., 2014) as part of the warm phase of the Atlantic Multidecadal Variability in the past decades. Remote effects of cooling or suppressed warming in the Southern Ocean (Y. Dong et al., 2022) is another proposed mechanism.

Given the wide range of explanations and potential interplay between variability and forced signal, the overarching goal of the present study is to provide new insights into the recent decadal strengthening of the Walker circulation. Using a broad range of indices based on different physical variables updated with the most recent data, including their spatial trends, reveals nuances that a single index cannot capture, helping to reduce uncertainty concerning whether a trend exceeds natural variability or not. Our further goal is to extract a pattern from the observed SST trends that is not associated with either the PDO signal or the uniform warming trend, and to

compare this pattern and related Walker circulation changes to those generated by CMIP6 models. We refer to this residual pattern, presumably anthropogenically forced, as the Northern Hemisphere-Indo-West Pacific warming pattern (NH-IWP). We then compare it to the transient ocean-thermostat pattern simulated by a subset of CMIP6 models in a range of realistic and idealized global warming simulations and discuss the key mechanisms involved.

2. Methods

2.1. Pacific Walker Circulation Indices

To evaluate recent changes to the Pacific Walker cell, we use eight indices based on different physical variables all reflecting the strength of the Walker circulation from a combination of satellite, reanalysis and blended data sets (ESR, 2009; Huang et al., 2017; Kalnay et al., 1996; Lee, 2014; P. Xie & Arkin, 1997; Zlotnicki et al., 2019). These data sets are summarized in Supplementary Table 1 and Supplementary Figure 1 in Supporting Information S1.

2.2. Decomposition of Observed SST Trends

To compare the observed SST trends of the last 40 years with natural decadal variability in the Pacific, we define the PDO following d'Orgeville and Peltier (2007). We smooth the SST monthly data using a 5-year rolling mean to eliminate shorter interannual variability. Then we take SST anomalies from 1920 until 2021 and compute the first and second Empirical Orthogonal Functions (EOFs) for the North Pacific region defined as 20° to 65°N, 120° to 260°E. To obtain the global PDO pattern, we regress the smoothed SST data for the same period onto the principal component timeseries corresponding to the second EOF for the North Pacific, while the first EOF describes a nearly uniform warming in that region.

Next, we calculate a spatially uniform linear warming trend T_0, in °C/decade, from 1980 to 2021 in the region 65°S to 65°N, and subtract it from the observed full trend pattern. By construction, the obtained anomalies have a zero spatial mean. We then compute a spatial linear regression of those anomalies onto the already obtained PDO pattern by computing coefficient a, having units of decade^{-1}, which minimizes the difference between the PDO pattern multiplied by a and these anomalies. The residual, obtained by subtracting a*PDO from the trend anomalies, is not associated with the PDO pattern nor with the uniform global warming. In summary, the trends are represented as:

$$\text{Trends}_{\text{lat,lon}} = T_0 + a \cdot \text{PDO}_{\text{lat,lon}} + \text{residual}_{\text{lat,lon}}$$

Our main results are based on ERSSTv5, but we repeat this analysis for the COBE (Ishii et al., 2005), HadISST (Rayner et al., 2003) and KAPLAN (Kaplan et al., 1998) data sets as well (Supplementary Table 1 caption and Supplementary Figures 6–8 in Supporting Information S1).

2.3. CMIP6 Model Simulations

While some previous studies have applied the large-ensemble approach to assess the simulation of the Walker circulation trends (e.g., Seager et al., 2022; Wills et al., 2022), here we use a complementary approach focusing on a broader selection of models, albeit with fewer ensemble members. To compare the observed trends with a broad range of climate simulations, we consider 40 different models from the CMIP6 archive for which surface temperature (ts), sea-level pressure (SLP) (psl) and surface winds (uas) are available for the historical simulations (Eyring et al., 2016 and Supplementary Figure 2 in Supporting Information S1). To give each model equal weight, we first utilize only one ensemble member per model. Next, to compare trends and natural variability, we assess the historical trends simulated by the models that have three or more ensemble members available.

Following Heede and Fedorov (2021), we then select a subset of models that have the strongest transient OT response to global warming in idealized CO_2 scenarios (here referred to as OT models, Supplementary Figure 2 in Supporting Information S1). They are selected based on the criterion that their Indo-Pacific SST gradient increases by at least 0.25°C relative to the piControl experiment during the first 25 years of the abrupt 4xCO_2 experiment. We also define another model subset that includes models developing a pronounced eastern EP warming pattern in the same experiment (EP models, Supplementary Figure 2 in Supporting Information S1).

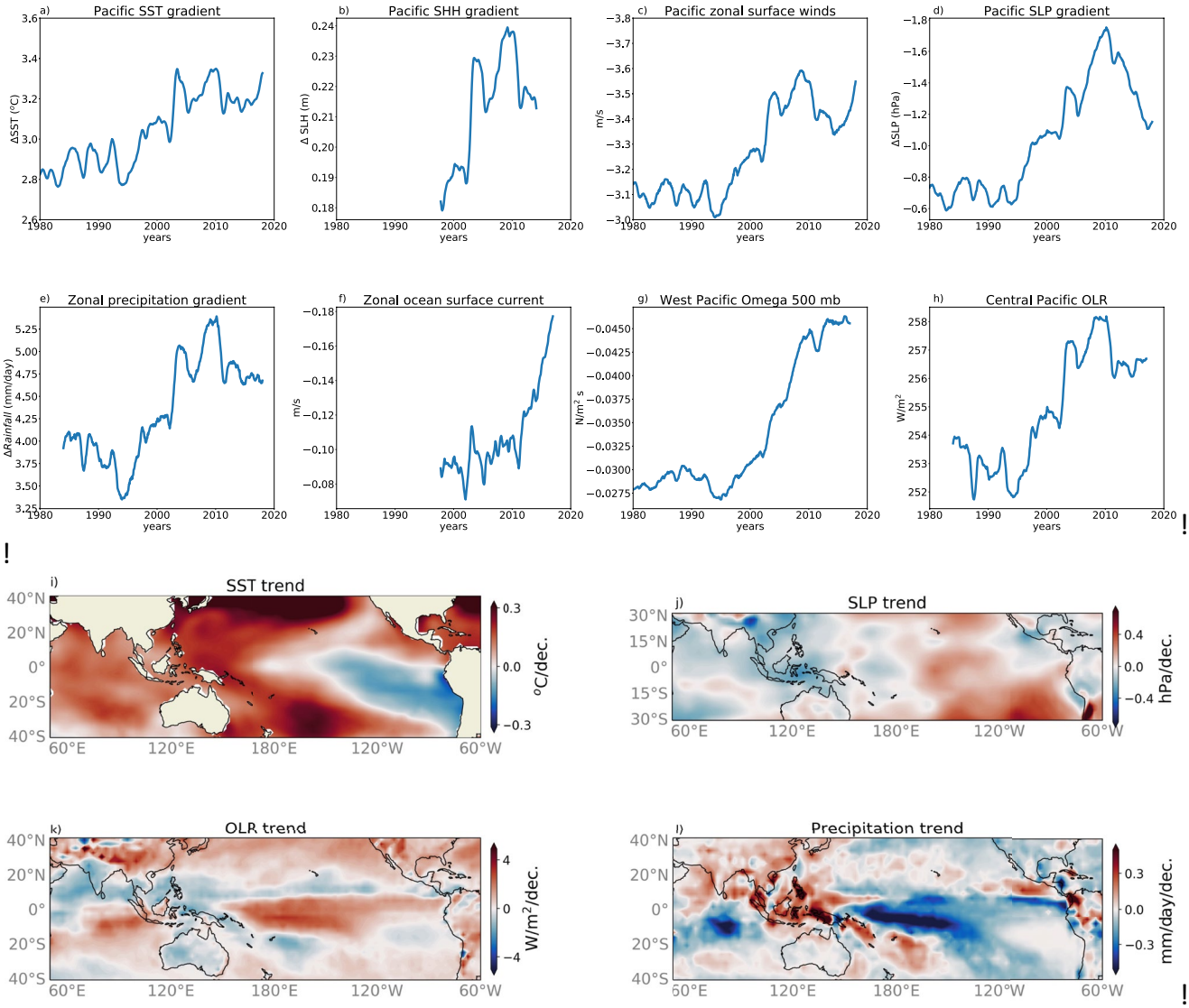

Figure 1. Temporal and spatial changes of the Pacific Walker circulation between 1980 and 2021 reflected in different atmospheric and oceanic variables (a–h) Climate indices for the Walker circulation. A 10-year running mean is applied (i–l) Maps of local linear trends in sea surface temperature (SST), sea-level pressure (SLP), outgoing longwave radiation and precipitation showing the spatial structure of changes associated with the strengthening of the Walker circulation in the tropical Indo-Pacific. Note the cooling of the eastern equatorial Pacific and of a broad region off the coast of South America, resulting in a significant increase in the east–west SST and SLP gradients along the equator. The metrics and datasets used here are described in Methods and Table 1 in Supporting Information S1.

Finally, we repeat the decomposition of historical SST trends replicated by one CMIP6 model, CESM2-FV2, which shows a strong late 20th century Walker circulation strengthening across three ensemble members, as measured by the zonal SST gradient strength, and compare the resulting patterns with those obtained from the observations.

3. Results

3.1. Forty-Year Trends of the Pacific Walker Circulation

Figures 1a–1h shows a clear decadal strengthening of the Walker circulation, as reflected in a variety of physical variables and robust across all indices since the 1990s. In most variables, the trend appears to be strongest between the El Niño events of 1997 and 2015. The trend is more pronounced in the SLP gradient than the SST gradient. Between years 2016–2021, the trend does not continue for the majority of indices. For some indices such as SLP

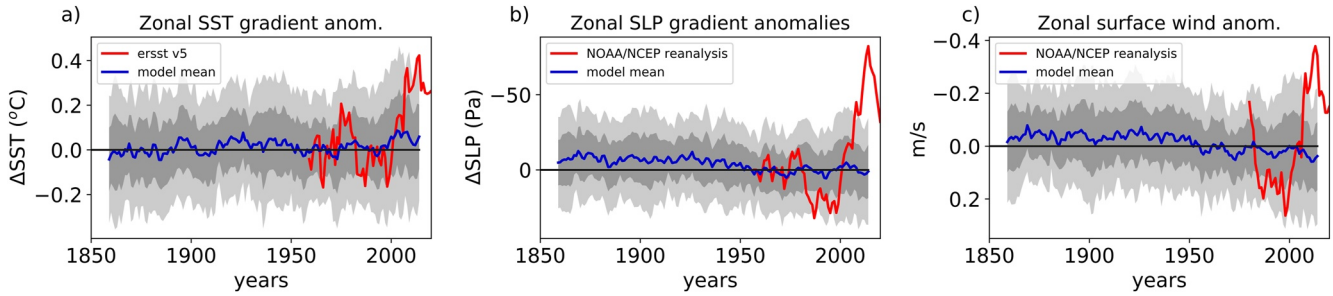

Figure 2. Observed and simulated historical variations in the east–west sea surface temperature (SST) gradient, sea-level pressure (SLP) gradient and zonal surface winds along the equator. Anomalies relative to a baseline are plotted. Observations are in red; a multi-model mean of CMIP6 models is in blue. The model spread across the 40 CMIP6 models is indicated by dark and light gray shadings (one and two standard deviations, respectively). A 10-year running mean is applied before calculating the spread. The observed anomalies of the past decades stay within models' two standard deviations for the zonal SST gradient (average z-score of 1.45 between 2005 and 2015) but exceed two standard deviations for the SLP gradient (z-score of 2.83) and zonal winds (z-score of 2.1). Note the reverse vertical axes for Figures 3b and 3c. Baseline values were computed for each model and the observations, and then subtracted from the data. The baseline calculations cover the period from 1950 to 1970 for SST and SLP gradients and from 1980 to 1985 for zonal surface wind anomalies as the wind data is less reliable prior to this period. For details see Methods and Table 1 in Supporting Information S1.

and sea surface height, it appears to reverse the sign, while for some other indices, including outgoing longwave radiation (OLR) and pressure velocity (Omega), the trend plateaus. Yet, for the zonal equatorial current speed the trend continues after 2015. These differences preclude us from concluding whether the multi-decadal Walker cell strengthening trend has resumed or stopped after 2015.

Examining spatial changes contributing to the Walker circulation trends (Figures 1i–1l), we highlight a pronounced cooling in the Pacific SST since the 1980s that is located primarily in the eastern and central EP and in a broad region south of the equator adjacent to South America. SLP trends show decreasing pressure over the Maritime continent but increasing pressure in the central-eastern EP. Correspondingly, precipitation and OLR trends show an increase in precipitation (decrease in OLR) over the Maritime continent, and a decrease in precipitation (increase in OLR) across the Pacific (Figures 1k and 1l). All these changes imply the Walker circulation intensification and the corresponding strengthening of Pacific trade winds.

3.2. Comparison Between the Observed and CMIP6 Model Walker Cell Trends

Examining three key indices for the Walker circulation strength in Figure 2 (zonal SST gradient, SLP gradient, and surface winds along the equator), we find that the observed anomalies in the SST gradient reach, but do not exceed two standard deviations of the CMIP6 multi-model spread, with an average z-score, measured in terms of standard deviations from the mean, of 1.45 between 2005 and 2015. Both the SLP gradient and surface wind index do exceed two standard deviations during the peak of the Walker circulation strengthening trend with z-scores of 2.83 and 2.10, respectively, for the same interval. Together these findings demonstrate that the observed Walker cell trends cannot be replicated by CMIP6 models at large.

When analyzing individual models, we find that the observed SST gradient changes remain within natural variability in several CMIP6 models, see Supplementary Figure 3 in Supporting Information S1. However, the observed SLP gradient changes lie outside the range of natural variability for all the models considered (Supplementary Figure 4 in Supporting Information S1). These results, based on three ensemble members for each model, are generally consistent with large-ensemble simulations (Seager et al., 2022; Wills et al., 2022).

We have identified one model (CESM2-FV2) that has a late twentieth—early 21st century Walker cell strengthening trend *exceeding* the observed trend between 1970 and 2019 in terms of the zonal SST gradient, yet still underestimating the SLP gradient changes (Supplementary Figure 5 in Supporting Information S1). The spatial patterns of trends in the tropical Pacific in this model are qualitatively similar to the observed in Figure 1 (see Supplementary Figure 11 in Supporting Information S1). However, at the same time, this model shows cooling in the Indian ocean and a weaker warming in the South Pacific, driving SLP anomalies in those regions different from the observed.

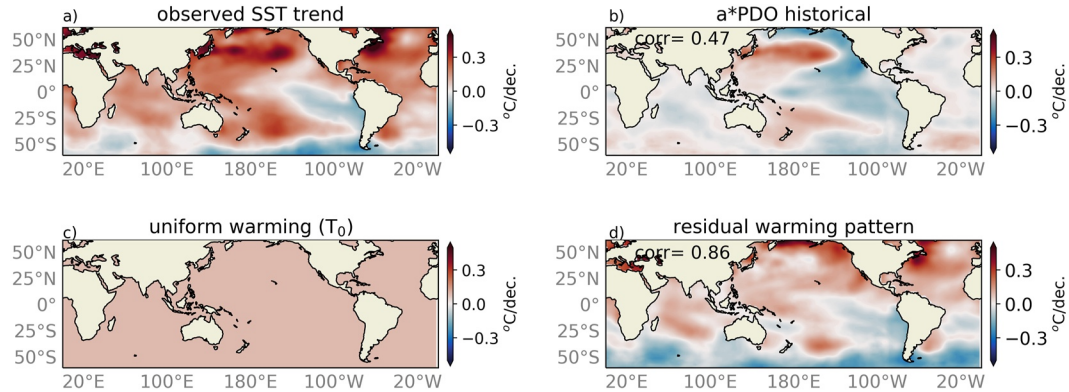

Figure 3. Decomposing the observed sea surface temperature (SST) trends into key components. (a) The global pattern of the observed local SST trends for years 1980–2020. This pattern is partitioned into three components: (b) a weighted negative Pacific Decadal Oscillation (PDO) pattern; (c) a spatially uniform warming trend T_0; and (d) the residual trend pattern once the PDO signal and uniform warming have been subtracted from the full SST pattern. We refer to the residual, in the global context, as the Northern Hemisphere-Indo West Pacific (NH-IWP) warming pattern. Its equatorial signature contributes to the weakening of the Walker cell. The computation of historical PDO is described in Methods. The weight coefficient "a" is obtained by a least-squares fit between the PDO pattern and the full trend map minus uniform warming. Correlation coefficients provided in panels (b and d) indicate the spatial correlation between a given pattern and the full SST warming pattern with the uniform warming subtracted (i.e., panel a minus (c)) between 60°S and 60°N.

3.3. Decomposing SST Trend Pattern Into a PDO Signal and a Residual

We next decompose the observed SST trend pattern (as a function of latitude and longitude) into the PDO signal, a spatially uniform warming and a non-PDO residual (Figure 3). These three signals have all comparable magnitudes. Importantly, the eastern-central Pacific equatorial cooling and enhanced warming of the West Pacific and Indian oceans persist in the residual SST pattern (Figure 3d). In addition, it shows a clear interhemispheric asymmetry with a greater warming in the Northern Hemisphere and cooling in the Southern Hemisphere. Therefore, we refer to the residual as the NH-IWP. Its structure is mostly similar across different datasets (Supplementary Figures 6–8 in Supporting Information S1). Its origin will be discussed next.

3.4. Comparison of SST Patterns Between Observations and CMIP6 Models

To understand the origin of the NH-IWP warming pattern, that is, the non-PDO residual, we turn to the subset of CMIP6 models with a strong OT response (the OT model category, Methods). Figure 4 compares the observed residual trends to SST anomalies simulated by OT model subset in idealized and historical experiments. The residual trend pattern looks remarkably similar to the first decade of the abrupt-4xCO_2 SST response to the forcing in OT models both in terms of the Southern Hemisphere cooling and tropical Indo-Pacific temperature gradient (Figure 4b), with a pattern correlation of 0.68. Qualitatively, it also looks similar to SST anomalies in the gradual 1pctCO_2 and historical simulations (Figures 4c and 4d) by OT models, even though the Indian ocean warming is weaker, and hence the resulting strengthening of the Indo-Pacific temperature gradient is smaller than in the observations.

Overall, the similarity between the NH-IWP pattern and the transient SST response to global warming in this subset of models suggests that this pattern is part of the climate system forced response to radiative forcing. Moreover, since we selected this subset on the basis of the relatively strong transient increase in the equatorial east–west SST gradient (hence the OT name), the equatorial signature of the NH-IWP pattern likely reflects the ocean thermostat mechanism of the tropical Indo-Pacific response to global warming. Nevertheless, additional contributions from other sources to this equatorial signal, such anthropogenic aerosols (Heede & Fedorov, 2021) or remote effects of ozone depletion in the Southern Hemisphere (Hartmann, 2022) cannot be excluded.

Supplementary Figures 9 and 10 in Supporting Information S1 compares warming SST trends averaged for different regions of the tropical ocean basins in the observations and in CMIP6. It is evident that the CMIP6 models consistently underestimate warming in the Indian Ocean by about 0.3 K on average since 1950 with the observed trend outside two standard deviations of the CMIP6 model mean trend (average z-score of 2.16 between 1960 and

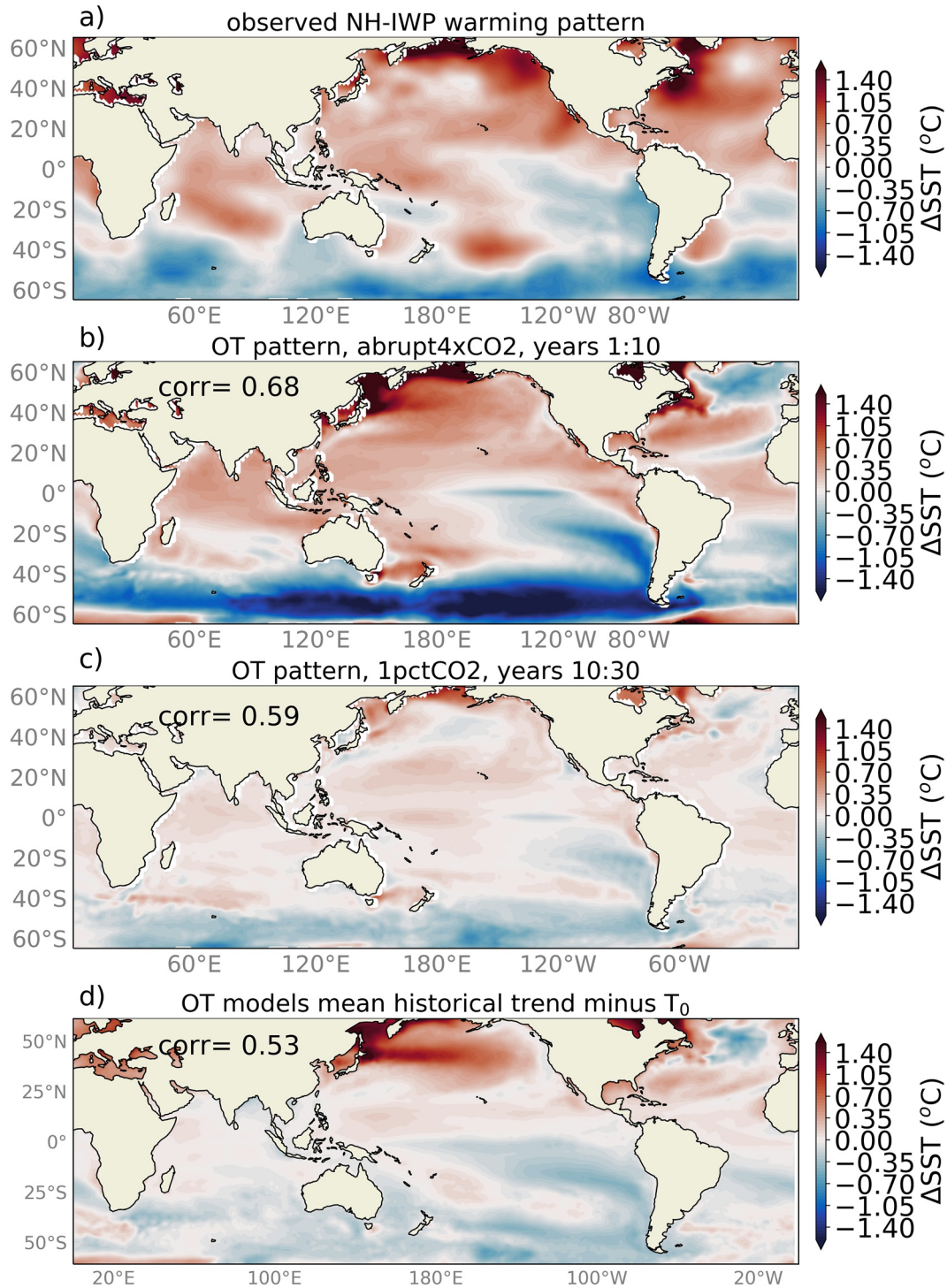

Figure 4. Comparison between the observed Northern Hemisphere-Indo-West Pacific warming pattern (NH-IWP) warming pattern and sea surface temperature (SST) anomalies in three types of experiments using ocean-thermostat-like (OT) models. (a) The observed NH-IWP SST pattern trend (i.e., the residual pattern in Figure 3d). multiplied by four decades. (b) SST anomalies for the first 10 years of the abrupt-4xCO_2 experiment relative to the piControl experiment averaged across OT models. (c) SST anomalies relative to piControl for years 10–30 in the 1pctCO_2 experiment for OT models. (d) Historical trends simulated by OT models for years 1980–2015 multiplied by 3.5 decades. Mean warming is subtracted from panels (b–d). The OT category is defined as the subset of CMIP6 models that develop a relatively strong ocean thermostat (Methods). Correlation coefficients provided in panels (b–d) indicate the spatial correlation between the given pattern and the NH-IWP warming pattern in panel (a) between 60°S and 60°N.

2015). Simultaneously, the CMIP6 models overestimate the North Pacific warming between 1970 and 2000. The observed Atlantic warming is captured well by the models, while both the East and West Pacific warming is, on average, underestimated by the models, but remains within two standard deviations.

For the CESM2-FV2 model, whose SST gradient trend exceeds the observed trend, we complete the same trend pattern partitioning as in Figure 3 but for the period of the model's historical simulation during which the Walker circulation increase is the strongest (Supplementary Figures 11 and 12 in Supporting Information S1). For this particular model, the PDO and uniform warming signals are generally similar to the observations (Figure 3). The residual warming pattern however has both similarities and differences. In particular, the ocean does cool in the eastern EP and off the South American coast, strengthening the east–west Pacific SST gradient. Thus, pattern is critical for the Walker circulation strengthening. However, there is no enhanced Indian Ocean warming relative to the mean warming, which is markedly different from the observations. The North Pacific warming and inter-hemispheric asymmetry appear stronger in CESM2-FV2 than in the CMIP6 average.

4. Discussion and Conclusions

A multi-variable assessment of the Pacific Walker circulation changes since the 1980s shows a robust decadal strengthening trend, particularly pronounced from the early 1990s to 2015. This trend is accompanied by SST cooling along equator in the central-eastern Pacific and off the coast of South America, a pronounced deepening of low pressure and increased precipitation over the Maritime continent, and a general precipitation decrease over most of the EP Ocean.

The full pattern of ocean warming shares some similarities with the negative PDO pattern, but is distinct from the PDO in several aspects, including the enhanced warming of the Northern Hemisphere and of the Indian Ocean. This is highlighted by our decomposition of the signal into a spatially uniform warming, the PDO signal, and a non-PDO residual, all of which having similar magnitudes. It is the residual pattern that shows an enhanced NH-IWP warming, as well as cooling of the central-eastern equatorial and southeastern regions of the Pacific Ocean. In addition, the NH-IWP warming pattern includes cooling or suppressed warming in the Southern Ocean, which can reinforce changes in the tropical Pacific (Y. Dong et al., 2022). Consequently, the increased equatorial Indo-Pacific SST gradient and greater interhemispheric asymmetry compared to the PDO suggest that the observed decadal trends in the Walker circulation cannot be explained solely by the transition from a positive to a negative PDO phase.

One of our key findings is that the residual trend pattern isolated in the observations, that is, the NH-IWP pattern, closely resembles the transient pattern that the OT subset of CMIP6 models generates in the Indo-Pacific during the first decades of the abrupt-4xCO_2 experiments. OT models also capture this pattern in historical simulations but only partially, underestimating Indian ocean warming and the overall strength of the signal. Simulating this pattern is even more problematic for the EP models, which tend to quickly generate an eastern EP warming (Supplementary Figure 14 in Supporting Information S1). This implies that CMIP6 models at large may be missing or underestimating the transient forced response to global warming critical for the strengthening of the Walker cell. Eventually, the Walker cell is expected to weaken by century-end (DiNezio et al., 2013; Heede & Fedorov, 2021; Kang et al., 2020; Wu et al., 2021; Xie et al., 2010). However, coupled GCM experiments show that the timing of emergence and magnitude of the future weakening critically depends on the strength of the transient OT response to global warming (Heede & Fedorov, 2021; Lu et al., 2021; also see Ying et al., 2022).

Our results indicate that on the whole the transient OT response is underestimated and/or distorted in climate models, raising questions on the accuracy of model projections for the tropical Pacific. We note that for adaptation and mitigation purposes the transient adjustment of the climate system to rising atmospheric GHGs is of greater importance in the near-term than the equilibrium response. Hence, studying the transient adjustment of the climate system and further understanding what drives discrepancies between the observations and historical simulations ought to be a major research focus.

The tendency to underestimate the Indian Ocean warming is a general issue among the CMIP6 models, as the observed trend lies outside two standard deviations of the multi-model average. In particular, this issue could explain why the models fail to capture the observed SLP and surface wind trends, since enhanced Indian Ocean warming would strengthen Pacific trade winds (L. Dong & McPhaden, 2018). In turn, underestimating Indian Ocean warming can be related to model biases in mean winds, atmospheric convection and

clouds, and/or oceanic mixed layer. It is noteworthy however that it may be possible to replicate the observed strengthening of the east–west SST gradient, but not the SLP gradient, without capturing the trans-basin warming trends, provided the model can generate a strong asymmetric mode in the Pacific (the example below).

Among climate models analyzed, we find one model (CESM2-FV2) that shows a late 20th century trend similar to the observed in the 21st century in terms of changes in the east–west equatorial SST gradient. In this model we see both a negative PDO pattern and a strong externally-forced mode. However, the latter shows a cooling signal in the Indian ocean (relative to the mean warming), which leads to somewhat different spatial trend patterns in SLP and precipitation and hence the model's inability to fully capture the observed trend in the zonal SLP gradient. Nevertheless, the simulated NH-IWP pattern (albeit modified) has similarities with that in the observations, and it is the simultaneous occurrence of this pattern and the negative PDO that helps simulate the strengthening of the Walker circulation in this model. This example also suggests that models may have a residual warming pattern capturing some features of the observations, while still underestimating the Walker cell strengthening.

Wu et al. (2021) and Olonscheck et al. (2020) argue that large ensemble simulations can capture the observed strengthening of the Pacific Walker circulation, which would require having an ensemble member with a sufficiently strong negative phase of the PDO. However, Wills et al. (2022) and Seager et al. (2022) find, the probability that the model internal variability can indeed account for the trends is very low. Here, we compliment the latter studies by showing that the PDO alone is also not sufficient to describe the spatial structure of the observed SST, SLP and surface wind trends. Another mode is needed, that is, the NH-IWP warming pattern. We suggest that the NH-IWP warming pattern is primarily a forced response to an increase in atmospheric GHGs.

However, we acknowledge that there could be possible contribution from other modes of natural variability and change, such as those originating in the Atlantic (Hu & Fedorov, 2018; Kucharski et al., 2011; Levine et al., 2017; X. Li et al., 2016; McGregor et al., 2014) or the Southern Annular Mode influenced by ozone depletion (Hartmann, 2022). However, while CMIP6 historical simulations capture the tropical Atlantic warming for example, they do not generate the strengthening of the Pacific zonal gradients (Supplementary Figure 9 in Supporting Information S1).

We further note that some studies have suggested that the observed PDO pattern may have an externally forced component (i.e., L. Dong et al., 2014), possibly associated with atmospheric aerosols. However, we argue that regardless of the extent to which the PDO may be forced, there is a residual warming pattern in the observations, different from the negative PDO phase and characterized by enhanced Northern Hemisphere and Indian-Western Pacific ocean warmings as well as an enhanced zonal SST gradient along the equator. This mode is not fully captured by the historical simulations of CMIP6 models.

Finally, another issue related to the models' inability to capture the observed trends concerns the effect of aerosols on the warming patterns. Analyzing single-forcing model experiments, Heede and Fedorov (2021) have shown that aerosols on average delay the onset of eastern EP warming, and in several models induce an equatorial cooling that counteracts the EP warming seen in GHG-only experiments. The spatial structure of cooling due to aerosols is however different from the NP-IWP pattern and hence the relative role of aerosols versus GHGs in driving the externally-forced warming pattern remains uncertain. Nevertheless, the expected decline in anthropogenic aerosols may accelerate the emergence of the EP warming pattern.

Conflict of Interest

The authors declare no conflicts of interest relevant to this study.

Data Availability Statement

All CMIP6 data is available on https://esgf-node.llnl.gov/search/cmip6/. All observed data is available as stated in Supplementary Table 1 in Supporting Information S1. All code used for data analysis and figures is available online: https://github.com/ubbu36/Colder-eastern-equatorial-Pacific-and-stronger-Walker-circulation-in-the-early-21st-century-GRL/.

Acknowledgments
U.K.H. was supported by a NASA FINESST Fellowship (80NSSC20K1634). A.V.F. is supported by Grants from NASA (80NSSC21K0558) and NOAA (NA20OAR4310377). Additional funding is provided by the ARCHANGE project (ANR-18-MPGA-0001, France). We also acknowledge a generous gift to Yale University from T. Sandoz. The funders had no role in study design, data collection and analysis, decision to publish or preparation of the manuscript. We further acknowledge freely available observational data sets provided by NOAA PSL, NASA PO.DAAC and the Met Office Hadley Centre.

References

Bjerknes, J. (1969). Atmospheric teleconnections from the equatorial Pacific. *Monthly Weather Review*, *97*(3), 163–172. https://doi.org/10.1175/1520-0493(1969)097<0163:atftep>2.3.co;2

Burls, N. J., & Fedorov, A. V. (2014). What controls the mean east–west sea surface temperature gradient in the equatorial Pacific: The role of cloud Albedo. *Journal of Climate*, *27*(7), 2757–2778. https://doi.org/10.1175/jcli-d-13-00255.1

Chou, C., Neelin, J. D., Chen, C.-A., & Tu, J.-Y. (2009). Evaluating the "rich-get-richer" mechanism in tropical precipitation change under global warming. *Journal of Climate*, *22*(8), 1982–2005. https://doi.org/10.1175/2008JCLI2471.1

Chung, E.-S., Timmermann, A., BrianSoden, J., Ha, K.-J., Shi, L., & John, V. O. (2019). Reconciling opposing Walker circulation trends in observations and model projections. *Nature Climate Change*, *9*(5), 405–412. https://doi.org/10.1038/s41558-019-0446-4

Clement, A. C., Seager, R., Cane, M. A., & Zebiak, S. E. (1996). An ocean dynamical thermostat. *Journal of Climate*, 9(9), 2190–2196. https://doi.org/10.1175/1520-0442(1996)009<2190:aodt>2.0.co;2

Coats, S., & Karnauskas, K. B. (2017). Are simulated and observed twentieth century tropical Pacific sea surface temperature trends significant relative to internal variability? *Geophysical Research Letters*, *44*(19), 9928–9937. https://doi.org/10.1002/2017gl074622

DiNezio, P. N., Clement, A. C., Vecchi, G. A., Soden, B. J., Kirtman, B. P., & Lee, S.-K. (2009). Climate response of the equatorial Pacific to global warming. *Journal of Climate*, *22*(18), 4873–4892. https://doi.org/10.1175/2009jcli2982.1

DiNezio, P. N., Kirtman, B. P., Clement, A. C., Lee, S.-K., Vecchi, G. A., & Wittenberg, A. (2012). Mean climate controls on the simulated response of ENSO to increasing greenhouse gases. *Journal of Climate*, *25*(21), 7399–7420. https://doi.org/10.1175/JCLI-D-11-00494.1

DiNezio, P. N., Vecchi, G. A., & Clement, A. C. (2013). Detectability of changes in the Walker circulation in response to global warming. *Journal of Climate*, *26*(12), 4038–4048. https://doi.org/10.1175/jcli-d-12-00531.1

Dong, L., & McPhaden, M. J. (2018). Unusually warm Indian Ocean sea surface temperatures help to arrest development of El Niño in 2014. *Scientific Reports*, *8*(1), 1–10. https://doi.org/10.1038/s41598-018-20294-4

Dong, L., Zhou, T., & Chen, X. (2014). Changes of Pacific decadal variability in the twentieth century driven by internal variability, greenhouse gases, and aerosols. *Geophysical Research Letters*, *41*(23), 8570–8577. https://doi.org/10.1002/2014GL062269

Dong, Y., Armour, K. C., Battisti, D. S., & Blanchard-Wrigglesworth, E. (2022). Two-way teleconnections between the Southern Ocean and the tropical Pacific via a dynamic feedback. *Journal of Climate*, *35*(19), 2667–2682. https://doi.org/10.1175/jcli-d-22-0080.1

d'Orgeville, M., & Peltier, W. R. (2007). On the Pacific decadal oscillation and the Atlantic multidecadal oscillation: Might they be related? *Geophysical Research Letters*, *34*(23), L23705. https://doi.org/10.1029/2007GL031584

Douville, H., Voldoire, A., & Geoffroy, O. (2015). The recent global warming hiatus: What is the role of Pacific variability? *Geophysical Research Letters*, *42*(3), 880–888. https://doi.org/10.1002/2014GL062775

England, M. H., McGregor, S., Paul, S., Meehl, G. A., Timmermann, A., Cai, W., et al. (2014). Recent intensification of wind-driven circulation in the Pacific and the ongoing warming hiatus. *Nature Climate Change*, *4*(3), 222–227. https://doi.org/10.1038/nclimate2106

Erfani, E., & Burls, N. J. (2019). The strength of low-cloud feedbacks and tropical climate: A CESM sensitivity study. *Journal of Climate*, *32*(9), 2497–2516. https://doi.org/10.1175/jcli-d-18-0551.1

ESR. (2009). *OSCAR third degree Version 1*. PO.DAAC.

Eyring, V., Bony, S., Meehl, G. A., Senior, C. A., Stevens, B., Stouffer, R. J., & Taylor, K. E. (2016). Overview of the coupled model Intercomparison project phase 6 (CMIP6) experimental design and organization. *Geoscientific Model Development*, *9*(5), 1937–1958. https://doi.org/10.5194/gmd-9-1937-2016

Fedorov, A. V., NatalieBurls, J., Lawrence, K. T., & Peterson, L. C. (2015). Tightly linked zonal and meridional sea surface temperature gradients over the past five million years. *Nature Geoscience*, *8*(12), 975–980. https://doi.org/10.1038/ngeo2577

Hartmann, D. L. (2022). The Antarctic ozone hole and the pattern effect on climate sensitivity. *Proceedings of the National Academy of Sciences*, *119*(35), e2207889119. https://doi.org/10.1073/pnas.2207889119

Heede, U. K., & Fedorov, A. V. (2021). Eastern equatorial pacific warming delayed by aerosols and thermostat response to CO_2.

Heede, U. K., Fedorov, A. V., & Burls, N. J. (2020). Timescales and mechanisms for the tropical Pacific response to global warming: A tug of war between the ocean thermostat and weaker Walker. *Journal of Climate*, *33*(14), 6101–6118. https://doi.org/10.1175/JCLI-D-19-0690.1

Heede, U. K., Fedorov, A. V., & Burls, N. J. (2021). A stronger versus weaker Walker: Understanding model differences in fast and slow tropical Pacific responses to global warming. *Climate Dynamics*, *1–18*(9–10), 2505–2522. https://doi.org/10.1007/s00382-021-05818-5

Held, I. M., & Soden, B. J. (2006). Robust responses of the hydrological cycle to global warming. *Journal of Climate*, *19*(21), 5686–5699. https://doi.org/10.1175/jcli3990.1

Hu, S., & Fedorov, A. V. (2018). Cross-equatorial winds control El Niño diversity and change. *Nature Climate Change*, *8*(9), 798–802. https://doi.org/10.1038/s41558-018-0248-0

Huang, B., Thorne, P. W., Banzon, V. F., Boyer, T., Chepurin, G., Lawrimore, J. H., et al. (2017). *NOAA extended reconstructed sea surface temperature (ERSST), Version 5* (Vol. 30(20), pp. 8179–8205). NOAA National Centers for Environmental Information. https://doi.org/10.1175/jcli-d-16-0836.1

Ishii, M., Shouji, A., Sugimoto, S., & Matsumoto, T. (2005). Objective analyses of sea-surface temperature and marine meteorological variables for the 20th century using ICOADS and the Kobe collection. *International Journal of Climatology: A Journal of the Royal Meteorological Society*, *25*(7), 865–879.

Kalnay, E., Kanamitsu, M., Kistler, R., Collins, W., Deaven, D., Gandin, L., et al. (1996). The NCEP/NCAR 40-year reanalysis project. *Bulletin of the American Meteorological Society*, *77*(3), 437–472. https://doi.org/10.1175/1520-0477(1996)077<0437:tnyrp>2.0.co;2

Kang, S. M., Xie, S.-P., Shin, Y., Kim, H., Hwang, Y.-T., Stuecker, M. F., et al. (2020). Walker circulation response to extratropical radiative forcing. *Science Advances*, *6*(47), eabd3021. https://doi.org/10.1126/sciadv.abd3021

Kaplan, A., Cane, M. A., Kushnir, Y., Clement, A. C., Blumenthal, M. B., & Rajagopalan, B. (1998). Analyses of global sea surface temperature 1856–1991. *Journal of Geophysical Research*, *103*(C9), 18567–18589.

Knutson, T. R., & Manabe, S. (1995). Time-mean response over the tropical Pacific to increased C_O2 in a coupled oceanocean-atmosphere model. *Journal of Climate*, *8*(9), 2181–2199. https://doi.org/10.1175/1520-0442(1995)008<2181:tmrott>2.0.co;2

Kociuba, G., & Power, S. B. (2015). Inability of CMIP5 models to simulate recent strengthening of the Walker circulation: Implications for projections. *Journal of Climate*, *28*(1), 20–35. https://doi.org/10.1175/jcli-d-13-00752.1

Kosaka, Y., & Xie, S.-P. (2016). The tropical Pacific as a key pacemaker of the variable rates of global warming. *Nature Geoscience*, *9*(9), 669–673. https://doi.org/10.1038/ngeo2770

Kucharski, F., Kang, I.-S., Farneti, R., & Feudale, L. (2011). Tropical Pacific response to twentieth century Atlantic warming. *Geophysical Research Letters*, *38*(3), L03702. https://doi.org/10.1029/2010gl046248

Lee, H. T. (2014). Climate algorithm theoretical basis document (C-ATBD): Outgoing longwave radiation (OLR)—daily. NOAA's climate data record (CDR) Program (Vol. *46*). CDR-ATBD-0526.
Levine, A. F. Z., McPhaden, M. J., & Frierson, D. M. W. (2017). The impact of the AMO on multidecadal ENSO variability. *Geophysical Research Letters*, *44*(8), 3877–3886. https://doi.org/10.1002/2017gl072524
Li, R. L., Studholme, J. H. P., Fedorov, A. V., & Storelvmo, T. (2022). Precipitation efficiency constraint on climate change. *Nature Climate Change*, *12*(7), 642–648. https://doi.org/10.1038/s41558-022-01400-x
Li, R. L., Studholme, J. H. P., Fedorov, A. V., & Storelvmo, T. (2023). Increasing precipitation efficiency amplifies climate sensitivity by enhancing tropical circulation slowdown and eastern Pacific warming pattern. *Geophysical Research Letters*, *50*, e2022GL100836. https://doi.org/10.1029/2022GL100836
Li, X., Xie, S.-P., Gille, S. T., & Yoo, C. (2016). Atlantic-induced pan-tropical climate change over the past three decades. *Nature Climate Change*, *6*(3), 275–279. https://doi.org/10.1038/nclimate2840
Lu, K., He, J., Fosu, B., & Rugenstein, M. (2021). Mechanisms of fast Walker circulation responses to CO_2 forcing. *Geophysical Research Letters*, *48*(23), e2021GL095708. https://doi.org/10.1029/2021GL095708
Luo, J.-J., Sasaki, W., & Masumoto, Y. (2012). Indian Ocean Warming modulates Pacific climate change. *Proceedings of the National Academy of Sciences*, *109*(46), 18701–18706. https://doi.org/10.1073/pnas.1210239109
Luo, Y., Lu, J., Liu, F., & Liu, W. (2015). Understanding the El Niño-like oceanic response in the tropical Pacific to global warming. *Climate Dynamics*, *45*(7–8), 1945–1964. https://doi.org/10.1007/s00382-014-2448-2
Ma, S., & Zhou, T. (2016). Robust strengthening and westward shift of the tropical Pacific Walker circulation during 1979–2012: A comparison of 7 sets of reanalysis data and 26 CMIP5 models. *Journal of Climate*, *29*(9), 3097–3118. https://doi.org/10.1175/jcli-d-15-0398.1
Mantua, N. J., Hare, S. R., Zhang, Y., Wallace, J. M., & Francis, R. C. (1997). A Pacific interdecadal climate oscillation with impacts on salmon production. *Bulletin of the American Meteorological Society*, *78*(6), 1069–1080. https://doi.org/10.1175/1520-0477(1997)078<1069:apicow>2.0.co;2
McGregor, S., Stuecker, M. F., Kajtar, J. B., England, M. H., & Collins, M. (2018). Model tropical Atlantic biases underpin diminished Pacific decadal variability. *Nature Climate Change*, *8*(6), 493–498. https://doi.org/10.1038/s41558-018-0163-4
McGregor, S., Timmermann, A., Stuecker, M. F., England, M. H., Merrifield, M., Jin, F.-F., & Chikamoto, Y. (2014). Recent Walker circulation strengthening and Pacific cooling amplified by Atlantic warming. *Nature Climate Change*, *4*(10), 888–892. https://doi.org/10.1038/nclimate2330
McPhaden, M. J., Santoso, A., & Cai, W. (2020). *El Niño southern oscillation in a changing climate* (Vol. 253). John Wiley & Sons.
Meng, Q., Latif, M., Park, W., Keenlyside, N. S., Semenov, V. A., & Martin, T. (2012). Twentieth century Walker circulation change: Data analysis and model experiments. *Climate Dynamics*, *38*(9–10), 1757–1773. https://doi.org/10.1007/s00382-011-1047-8
Merlis, T. M., & Schneider, T. (2011). Changes in zonal surface temperature gradients and Walker circulations in a wide range of climates. *Journal of Climate*, *24*(17), 4757–4768. https://doi.org/10.1175/2011jcli4042.1
Newman, M., Alexander, M. A., Ault, T. R., Cobb, K. M., Deser, C., Di Lorenzo, E., et al. (2016). The Pacific decadal oscillation, revisited. *Journal of Climate*, *29*(12), 4399–4427. https://doi.org/10.1175/jcli-d-15-0508.1
Olonscheck, D., Rugenstein, M., & Marotzke, J. (2020). Broad consistency between observed and simulated trends in sea surface temperature patterns. *Geophysical Research Letters*, *47*(10), e2019GL086773. https://doi.org/10.1029/2019GL086773
Rayner, N. A., Parker, D. E., Horton, E. B., Folland, C. K., Alexander, L. V., Rowell, D. P., et al. (2003). Global analyses of sea surface temperature, sea ice, and night marine air temperature since the late nineteenth century. *Journal of Geophysical Research*, *108*(D14), 4407. https://doi.org/10.1029/2002JD002670
Seager, R., Cane, M., Henderson, N., Lee, D.-E., Ryan, A., & Zhang, H. (2019). Strengthening tropical Pacific zonal sea surface temperature gradient consistent with rising greenhouse gases. *Nature Climate Change*, *9*(7), 517–522. https://doi.org/10.1038/s41558-019-0505-x
Seager, R., Henderson, N., & Cane, M. (2022). Persistent discrepancies between observed and modeled trends in the tropical Pacific ocean. *Journal of Climate*, *35*(14), 4571–4584. https://doi.org/10.1175/JCLI-D-21-0648.1
Seager, R., & Murtugudde, R. (1997). Ocean dynamics, thermocline adjustment, and regulation of tropical SST. *Journal of Climate*, *10*(3), 521–534. https://doi.org/10.1175/1520-0442(1997)010<0521:odtaar>2.0.co;2
Shankle, M. G., Burls, N. J., Fedorov, A. V., Thomas, M. D., Liu, W., Penman, D. E., et al. (2021). Pliocene decoupling of equatorial Pacific temperature and PH gradients. *Nature*, *598*(7881), 457–461. https://doi.org/10.1038/s41586-021-03884-7
Sohn, B. J., Yeh, S.-W., Schmetz, J., & Song, H.-J. (2013). Observational evidences of Walker circulation change over the last 30 Years contrasting with GCM results. *Climate Dynamics*, *40*(7), 1721–1732. https://doi.org/10.1007/s00382-012-1484-z
Solomon, A., & Newman, M. (2012). Reconciling disparate twentieth-century Indo-Pacific ocean temperature trends in the instrumental record. *Nature Climate Change*, *2*(9), 691–699. https://doi.org/10.1038/nclimate1591
Sun, D.-Z., & Liu, Z. (1996). Dynamic Ocean-atmosphere coupling: A thermostat for the tropics. *Science*, *272*(5265), 1148–1150. https://doi.org/10.1126/science.272.5265.1148
Sun, D.-Z., Zhang, T., & Shin, S.-I. (2004). The effect of subtropical cooling on the amplitude of ENSO: A numerical study. *Journal of Climate*, *17*(19), 3786–3798. https://doi.org/10.1175/1520-0442(2004)017<3786:TEOSCO>2.0.CO;2
Tokinaga, H., Xie, S.-P., Timmermann, A., McGregor, S., Ogata, T., Kubota, H., & YukoOkumura, M. (2012). Regional patterns of tropical Indo-Pacific climate change: Evidence of the Walker circulation weakening. *Journal of Climate*, *25*(5), 1689–1710. https://doi.org/10.1175/jcli-d-11-00263.1
Vecchi, G. A., BrianSoden, J., Wittenberg, A. T., Held, I. M., Leetmaa, A., & Harrison, M. J. (2006). Weakening of tropical Pacific atmospheric circulation due to anthropogenic forcing. *Nature*, *441*(7089), 73–76. https://doi.org/10.1038/nature04744
Vecchi, G. A., & Soden, B. J. (2007). Global warming and the weakening of the tropical circulation. *Journal of Climate*, *20*(17), 4316–4340. https://doi.org/10.1175/jcli4258.1
Wara, M. W., & Delaney, M. L. (2005). Ana christina Ravelo, and Margaret L. DelaneyPermanent El Niño-like conditions during the pliocene warm period. *Science*, *309*(5735), 758–761. https://doi.org/10.1126/science.1112596
Watanabe, M., Dufresne, J.-L., Yu, K., Mauritsen, T., & Tatebe, H. (2020). Enhanced warming constrained by past trends in equatorial Pacific sea surface temperature gradient. *Nature Climate Change*, *11*(1), 33–37. https://doi.org/10.1038/s41558-020-00933-3
Wills, R. C. J., Levine, X. J., & Schneider, T. (2017). Local energetic constraints on Walker circulation strength. *Journal of the Atmospheric Sciences*, *74*(6), 1907–1922. https://doi.org/10.1175/JAS-D-16-0219.1
Wills, R. C. J., Yue, D., Proistosecu, C., Armour, K. C., & Battisti, D. S. (2022). Systematic climate model biases in the large-scale patterns of recent sea-surface temperature and sea-level pressure change. *Geophysical Research Letters*, *49*(17), e2022GL100011. https://doi.org/10.1029/2022GL100011

Wu, M., Zhou, T., Li, C., Li, H., Chen, X., Wu, B., et al. (2021). A very likely weakening of Pacific Walker circulation in constrained near-future projections. *Nature Communications*, *12*(1), 6502. https://doi.org/10.1038/s41467-021-26693-y

Xie, P., & Arkin, P. A. (1997). Global precipitation: A 17-year monthly analysis based on gauge observations, satellite estimates, and numerical model outputs. *Bulletin of the American Meteorological Society*, *78*(11), 2539–2558. https://doi.org/10.1175/1520-0477(1997)078<2539:gpayma>2.0.co;2

Xie, S.-P., Deser, C., Vecchi, G. A., Ma, J., Teng, H., & Wittenberg, A. T. (2010). Global warming pattern formation: Sea surface temperature and rainfall. *Journal of Climate*, *23*(4), 966–986. https://doi.org/10.1175/2009jcli3329.1

Ying, J., Collins, M., Cai, W., Timmermann, A., Huang, P., Chen, D., & Stein, K. (2022). Emergence of climate change in the tropical Pacific. *Nature Climate Change*, *12*(4), 356–364. https://doi.org/10.1038/s41558-022-01301-z

Zhang, L., Han, W., Karnauskas, K. B., Meehl, G. A., Hu, A., Rosenbloom, N., & Shinoda, T. (2019). Indian Ocean warming trend reduces Pacific warming response to anthropogenic greenhouse gases: An interbasin thermostat mechanism. *Geophysical Research Letters*, *46*(19), 10882–10890. https://doi.org/10.1029/2019gl084088

Zhang, Y., Wallace, J. M., & Battisti, D. S. (1997). ENSO-Like interdecadal variability: 1900–1993. *Journal of Climate*, *10*(5), 1004–1020. https://doi.org/10.1175/1520-0442(1997)010<1004:ELIV>2.0.CO;2

Zlotnicki, V., Zheng, Q., Willis, J., Ray, R., & Hausman, J. (2019). *MEaSUREs gridded sea surface height anomalies, Version 1812*. PO.DAAC.